

## Proton-Enhanced $^{13}\text{C}$ Imaging/Spectroscopy by Polarization Transfer

SCOTT D. SWANSON, LESLIE E. QUINT, AND HONG N. YEUNG\*

*Department of Radiology, University of Michigan Medical Center, Ann Arbor, Michigan 48109*

Received December 6, 1988; revised July 21, 1989

Carbon-13 magnetic resonance imaging/spectroscopy (CMRI/S) was performed using polarization transfer techniques where sensitivity of the carbon signal was enhanced by transferring the proton spin order to the carbon nuclei. The experimental feasibility of using polarization transfer techniques at 2.0 T was demonstrated with a phantom and an intact chicken egg. The potential clinical applications of CMRI/S with polarization transfer include the assessment of prostate cancer. Preliminary results using human prostate specimens are presented. © 1990 Academic Press, Inc.

### INTRODUCTION

The NMR signal of  $^{13}\text{C}$  is weak because of its low natural abundance (1.1%) and its low gyromagnetic ratio ( $\gamma_{\text{C}} \approx \gamma_{\text{H}}/4$ ). The large number of carbon atoms in biological moieties partly makes up for this insufficiency. The other difficulties commonly encountered with  $^{13}\text{C}$  NMR are the long  $T_1$ , the large chemical-shift dispersion, and the strong interactions (both dipolar interaction in solids and spin-spin couplings in liquids) with hydrogen nuclei with which the  $^{13}\text{C}$  atom is covalently bonded. Although each of these factors has an adverse effect on the carbon signal, one can manipulate the interactions between protons and carbons in a constructive way.

Enhancing the  $^{13}\text{C}$  signal by transferring the spin order from a high- $\gamma$  spin species (e.g., protons) to a nucleus with a low  $\gamma$  (e.g., carbons), coupled via heteronuclear dipole-dipole or spin-spin interactions, is a case in point. This cross-polarization is brought about through these otherwise undesirable interactions between the carbon and proton spins by establishing conditions which allow the proton spin order to be transferred to carbons. There are many methods of spin-order transfer (1). For fluid-like substances such as metabolites, two of the most common families of pulse technique for polarization transfer are known as INEPT (insensitive nuclei enhanced by polarization transfer) (2, 3) and DEPT (distortionless enhancement by polarization transfer) (4, 5).

In imaging applications, both chemical-shift and spatial information can be obtained by using a hybrid imaging/spectroscopy pulse sequence and then reconstructing the data with a multidimensional Fourier transform (6, 7). There are two serious problems in applying imaging techniques to  $^{13}\text{C}$ : the low sensitivity of the  $^{13}\text{C}$  nucleus

\* To whom all correspondence should be addressed.

and the higher magnetic gradient field strengths required to achieve the same spatial resolution as for protons (a factor of 4 greater). These two problems tend to compensate each other, however, since due to low sensitivity one can only obtain coarsely resolved  $^{13}\text{C}$  images. Because of these problems,  $^{13}\text{C}$  imaging and/or localized spectroscopy work has rarely been performed. Kormos *et al.* (8, 9) first demonstrated the feasibility of  $^{13}\text{C}$  imaging by obtaining proton-coupled  $^{13}\text{C}$  images at 4.7 T for phantoms and tissues. Recently, Sillerud *et al.* (10) formed carbon images on phantoms using indirect detection through protons, also at 4.7 T. Our goal in this study was to incorporate the polarization transfer techniques with the chemical-shift imaging sequence; in this manner many of the formidable problems associated with low- $\gamma$  nuclei, such as  $^{13}\text{C}$ , become easier and perhaps eventually solvable.

#### METHODS

The common idea of the INEPT and the DEPT techniques is to take advantage of the fact that the weak carbon (S spin) polarization is linked to a strong proton (I spin) polarization by a heteronuclear scalar interaction,  $J\text{I}\cdot\text{S}$ . The  $J_{\text{CH}}$  constant ranges from 120 to 180 Hz for compounds that are of interest to us. The pulse sequences of either of these two methods can be easily adapted for hybrid imaging/spectroscopy applications as shown in Fig. 1. The rf portion of the sequence in Fig. 1A is identical to the refocused INEPT sequence of Burum and Ernst (3). The factor of enhancement theoretically obtainable using the INEPT sequence depends upon the time delays  $\tau_1$  and  $\tau_2$  and the number of hydrogen atoms to which the carbon atom is covalently bonded. A reasonable compromise to achieve nearly equal polarization enhancements for  $-\text{CH}-$ ,  $-\text{CH}_2-$ , and  $-\text{CH}_3$  carbons is to set  $\tau_1 = (4J_{\text{CH}})^{-1}$  and  $\tau_2 = 1.5\tau_1$ . The actual enhancement one obtains on the basis of equal acquisition time can be, in effect, higher because of the (otherwise adverse) fact that the  $T_1$  of carbon is in general much longer than that of hydrogen. As a result, one can repeat the pulse sequence more often to accumulate the signal more rapidly than in the case of a conventional experiment. On the other hand, factors such as inhomogeneous rf fields or short transverse relaxation times (causing insufficient coherence transfer) can degrade the enhancement. While it is possible to exploit the functional dependence of signal amplitude on  $\tau_2$  to differentiate the  $-\text{CH}_n-$  groups ( $n = 1, 2, 3$ ) it is more natural to employ DEPT for this purpose.

The fundamental difference between INEPT and DEPT is that in the former case, the polarization transfer is carried through a  $J$ -order state which is a longitudinal two-spin order ( $I$ ), while in the latter case, it is through a heteronuclear multiple quantum coherence. The pulse sequence of a typical DEPT sequence can be illustrated by the rf section of the DEPT imaging/spectroscopy sequence as shown in Fig. 1B. In physical terms, the importance of polarization transfer stems from the fact that many of the formidable problems associated with low- $\gamma$  nuclei can be lessened by manipulating the magnetization of the bonded high- $\gamma$  nuclei, an easier task. Sensitivity enhancement is but one such example to the solution of these problems. Other examples include spatial-resolution enhancement through phase encoding via protons (indirect "spin warp") (11) and localization of carbon nuclei through indirect excitation upon protons (11, 12).

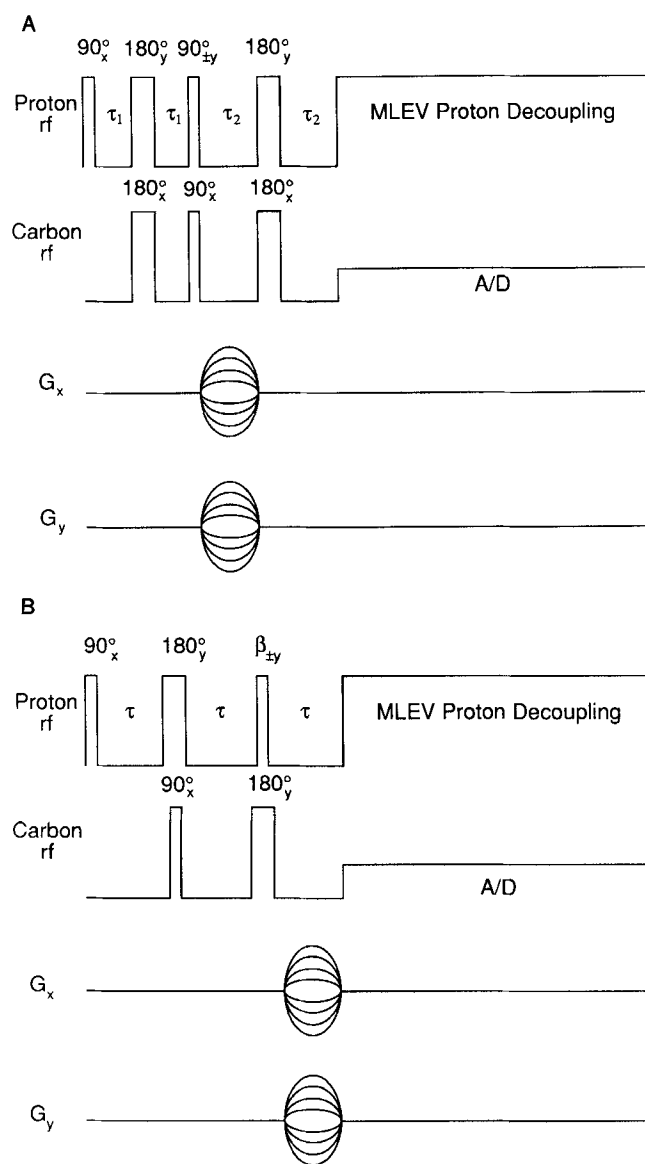


FIG. 1. Pulse sequences for  $^{13}\text{C}$  imaging/spectroscopy by polarization transfer with (A) refocused INEPT and (B) DEPT.

#### EXPERIMENTAL

Experiments were performed using a General Electric 2.0-T CSI system (31-cm bore diameter) equipped with a second rf channel for double resonance. The rf coils used were a separately tuned coil arrangement with a home-built carbon coil (four- to five-turn winding, cylindrical shape, 6-cm diameter) inside a 7-cm saddle-shaped

proton coil. The orthogonality requirement of these two coils was not found to be crucial. The proton decoupling scheme employed was a phase-alternated broadband MLEV sequence (13) provided by the manufacturer. Magnet shimming was performed before each experiment using the proton signal of the sample studied.

A three-tube phantom, an intact chicken egg, and five excised, intact human prostate specimens were used for this preliminary investigation. All samples had naturally abundant  $^{13}\text{C}$  isotopic composition. The three sample tubes in the phantom contained, respectively, ethylene glycol, lactic acid, and methanol. Two normal human prostate specimens were obtained from autopsies performed within 36 h of death. The three abnormal prostates were radical prostatectomy specimens obtained within minutes of surgical excision. All specimens were kept at ice temperature during transportation and all NMR scans started within an hour after specimen procurement.

The hybrid 3D (2D spatial and 1D spectral) data set on the three-tube phantom was obtained with the INEPT-like sequence shown in Fig. 1A, while the similar data set on the unfertilized egg was obtained with the DEPT technique in Fig. 1B. The tip angle of the rf pulse,  $\beta$ , in the DEPT sequence was set equal to  $45^\circ$ . For the prostate specimens, only total (unlocalized) spectra could be collected for the present study because of the limited time allocated for the study: all specimens had to be returned in 1–2 h for pathological analysis.

## RESULTS

To demonstrate the sensitivity enhancement, proton-decoupled spectra of the lactic acid sample obtained using conventional  $^{13}\text{C}$  spectroscopy and the INEPT technique of Fig. 1A are shown in Fig. 2. Both spectra in the figure were obtained with the same TR and the same number of accumulations. The sensitivity enhancement of the C2 carbon (a CH fragment) by the INEPT technique over the conventional technique is slightly less than 4. (One should bear in mind that the enhancement factor would be even higher, if we were to compare the results of conventionally acquired, proton-coupled spectra with those of proton-enhanced, proton-decoupled spectra, since proton-decoupling also can cause NOE enhancement in the conventional method.) The enhancement of the C3, methyl carbon signal is not as dramatic because of the particular choice of  $\tau_1$  and  $\tau_2$  (3).

There is more than one way to display a three-dimensional hybrid image/spectrum data set. In Fig. 3, the spectra of individual voxels of the three-tube phantom data is shown. Since the rf pulses were applied without any plane selection, the two spatial dimensions represent an image plane upon which intensities of each carbon species are projected along the cylindrical axis of each vial. We shall refer to this as a projection image plane. Out of the total 256 ( $16 \times 16$ ) pixels in this plane, only about 64 in the center of the field-of-view are shown. The voxel represents a sample volume of  $0.94 \times 0.94 \times h \text{ cm}^3$ , where  $h$  is the sample height. In the 4.5-cm-long sample vial used in this phantom, the number of  $^{13}\text{C}$  nuclei per voxel in ethylene glycol can be calculated to be approximately 1.56 mmol/voxel. The area occupied by each sample tube is approximately  $2 \times 2$  or 4 pixels. Because of the low spatial resolution, cross-pixel contamination of spectral components between the neighboring samples is unavoidable.

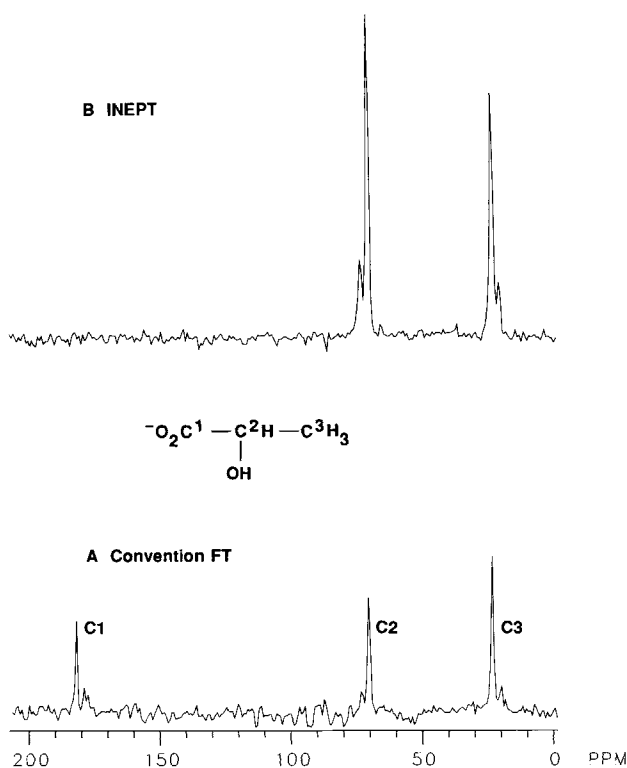


FIG. 2. Demonstration of sensitivity enhancement by polarization transfer in lactic acid.  $^{13}\text{C}$  spectra of lactic acid acquired (A) with a conventional one-pulse sequence and (B) with the refocused INEPT sequence. Both spectra were acquired with carbon and proton  $B_1$  fields of 2.0 kHz, 20 transient averages, and MLEV proton decoupling.

The results obtained by applying the DEPT imaging sequence of Fig. 1B on intact chicken egg are displayed in a different manner in Fig. 4. The nonlocalized  $^{13}\text{C}$ -NMR spectrum obtained with DEPT is shown in Fig. 4A, while Fig. 4B shows the  $^{13}\text{C}$  image projected along one of the minor axes of the egg ellipsoid and reconstructed from the methylene fragment of the  $^{13}\text{C}$  spectrum. *The methylene signal arises entirely from the yolk and therefore the image presented is of the yolk only.* Equivalent images, not shown here, of other carbon species which show sufficient signal-to-noise in the total spectrum can also be constructed. Signal from the proteins in the egg white are absent presumably due to the short  $T_2$  (of either  $^1\text{H}$  or  $^{13}\text{C}$ ) caused by the low mobility of its molecular constituents. Also absent are the unprotonated carbons such as carbonyls due to cancellation of carbon magnetization by the phase-cycling schemes commonly employed in polarization transfer.

Finally, Fig. 5 shows spectra of excised, intact human prostate specimens. The INEPT sequence was used with no spatial localization. Figure 5A is the spectrum of a normal gland and Fig. 5B is from a prostate with adenocarcinoma and underlying benign prostatic hypertrophy (BPH). These two spectra showed substantial and intriguing differences in chemical shifts. In this particular instance, the presence of a

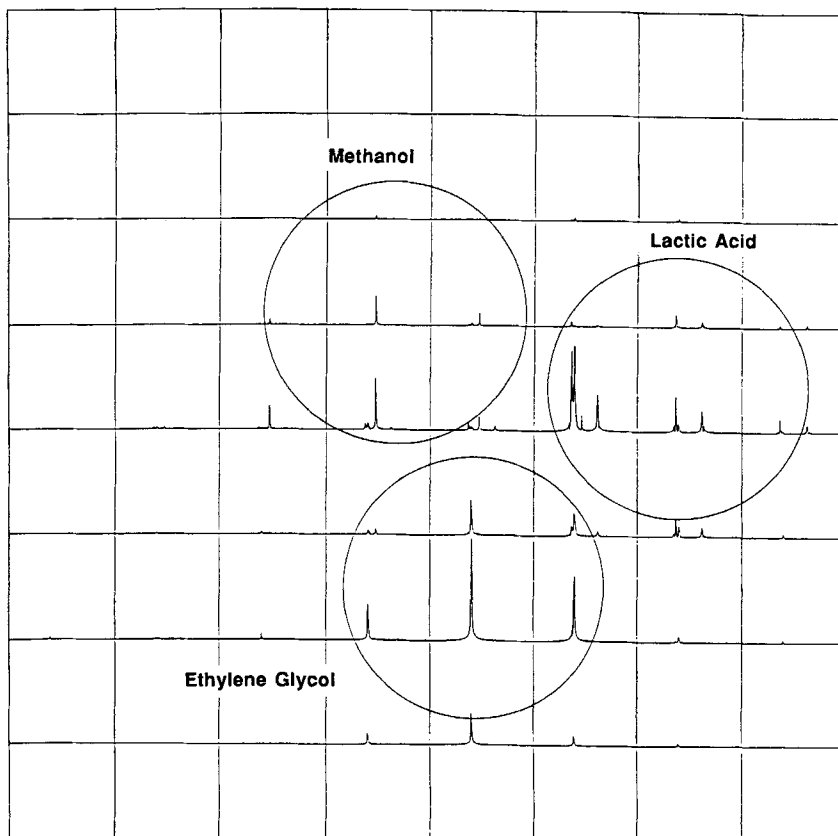


FIG. 3. Series of spatially resolved carbon spectra from the three-tube phantom consisting of methanol, lactic acid, and ethylene glycol collected with the refocused INEPT imaging pulse sequence of Fig. 1A. Each box represents a voxel and contains the  $^{13}\text{C}$  spectrum of the phantom from that particular voxel. The approximate positions of the vials in the phantom are shown by the circles. A total of 128 transient acquisitions for each of the  $16 \times 16$  phase-encoded, time-domain data sets were averaged with a pulse sequence repetition time of 500 ms. The field-of-view was  $150 \times 150$  mm and the total imaging time, 4.5 h. These data were reconstructed with a three-dimensional Fourier transform and 64 out of the 256 voxels are presented in magnitude mode in the figure.

prominent citrate peak near 45 ppm (with respect to TMS) in the prostate with underlying BPH as compared to the minute citrate peak of the normal gland seems to support the biochemical evidence cited by other investigators (see Discussion for references). However, we hasten to point out that our data are preliminary and are statistically inadequate to draw any conclusion. We intend to publish a full report after this study (which is still ongoing) is completed.

#### DISCUSSION

##### *Technical Issues*

While the INEPT and DEPT sequences both yield comparable signal enhancement over the conventional FT method, we found that the DEPT method is, in many

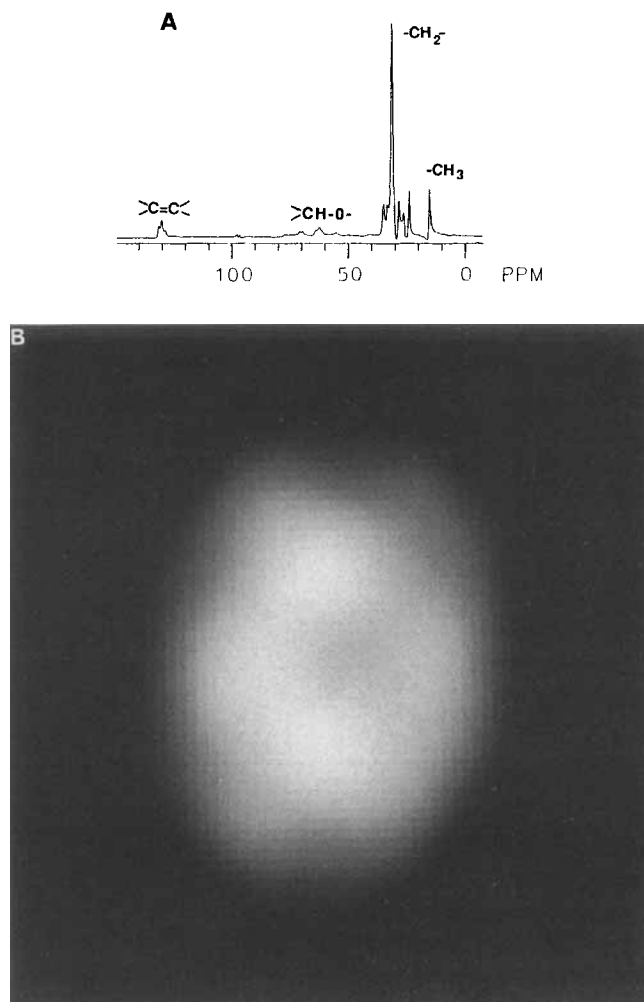


FIG. 4. (A) <sup>13</sup>C-NMR spectrum of an intact chicken egg obtained with the DEPT pulse sequence acquired with 436 transient averages, a duration of 3.85 ms for  $\tau$ , a 500-ms repetition rate and 90° pulsewidths of 125  $\mu$ s for the proton and carbon rf. The proton decoupling power was 4.9 W. (B) An image formed from the -CH<sub>2</sub>- component of the <sup>13</sup>C-NMR spectrum obtained with the DEPT chemical-shift imaging sequence of Fig. 1B acquired with 120 transient averages and a recycle time of 500 ms for a total imaging time of 4.3 h. The image in (B) was constructed by zero filling the 16  $\times$  16  $k$ -space array of the -CH<sub>2</sub>-resonance to an array of 128  $\times$  128 points and applying a two-dimensional Fourier transform to generate the two-dimensional spatial image.

respects, more convenient to use than the INEPT sequence. One of the reasons is that the time window between rf pulses required by the pulse sequences (see Figs. 1A and B) is less restrictive in the DEPT sequence [ $\tau = (2J_{\text{CH}})^{-1}$ ] than in the INEPT sequence [ $\tau_1 = (4J_{\text{CH}})^{-1}$ ]. Second, for rf pulses with nonideal tip angles, it is well known (14) that the rf sequences such as INEPT can generate an unintended zero quantum coherence which manifests itself as a zero-frequency or baseline artifact.

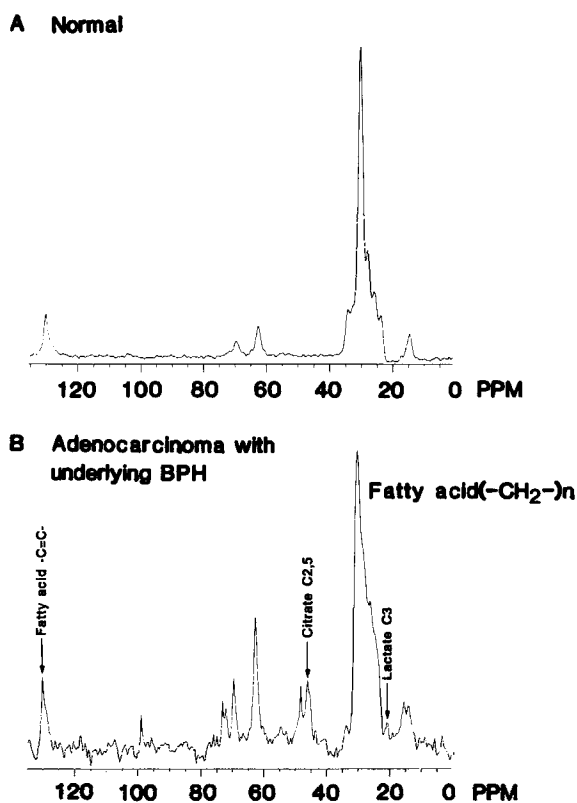


FIG. 5. Unlocalized  $^{13}\text{C}$  spectra of intact human prostate specimens. (A) Spectrum of a normal prostate gland acquired with 418 averages (6.9-min total acquisition time). (B) Spectrum of a specimen having adenocarcinoma with underlying BPH acquired with 1429 averages (23.8-min total acquisition time). Both spectra had a repetition rate of 500 ms and rf field strengths as in Fig. 4.

While this artifact can be corrected by proper phase adjustment during postprocessing (as in the data of our three-tube phantom), it is better to avoid the artifact entirely. This can be done at no cost using DEPT. Finally, as mentioned earlier, the sequence DEPT also provides a simple and straightforward way to perform spectrum editing by variation of the tip angle of the rf pulse  $\beta$ .

### *Biomedical Applications*

The application of  $^{13}\text{C}$  spectroscopy in studies of metabolism in tissue cells and organisms has been recognized for some time (15–19), particularly in studying glycogen and fat turnover in cell suspensions and whole organs (18, 20–25). So far most of the  $^{13}\text{C}$  high-resolution NMR studies of cells and organisms were performed at high fields with tissue samples or excised intact organs. Whole organs were scanned either with no attempt at localization or with the use of a surface coil; however, the degree of localization achievable with a surface coil is questionable.

The example of the whole-gland spectrum shown in Fig. 5 illustrates the problem of applying spectroscopic techniques without localization. There are biochemical



studies which show that the concentration of citrate increases in BPH and decreases in cancer-containing glands (26–28). Halliday *et al.* (29) postulated that prostate cancer might be detectable using naturally abundant CMRS to assess the level of citrate within a prostatic tissue sample. However, since foci of cancer and BPH often coexist in the same gland, the increased citrate signal from BPH-containing tissue may well obscure the lack of citrate signal from the nearby cancerous tissue. There may be other spectroscopic features that are more subtle and no less important. But it is clearly difficult to evaluate them unless the spectrum can be localized to smaller, anatomically definable regions. This is an endeavor we want to pursue in the immediate future before embarking on further clinical evaluations.

### *Clinical Feasibility*

The key question one should address with regard to the clinical feasibility of  $^{13}\text{C}$  magnetic resonance imaging/spectroscopy (CMRI/S) is “In what ways will these techniques become useful?” And, if an answer to this question has been found, “At what field strength will they become practical and safe?” We can only speculate on the answers to these questions based upon what little we presently know about the results on prostate cancer. The two most important issues with regard to the above questions are sensitivity and localization. The polarization transfer method, as mentioned earlier, offers improvements in both. Our experiments were conducted at 2.0 T, currently the highest-field MRI system in clinical use. While our present experimental arrangement can be improved in many ways, especially in sensitivity, it still may be an optimistic estimate of the *in vivo* situation which calls for the use of surface coil(s). We will not go into the problems of surface coils in this application. It is a complicated subject which has been touched upon by Norris *et al.* (12) using adiabatic pulses advocated by Ugurbil *et al.* (30). Sillerud *et al.* (31) recently showed a proton-coupled, *in vivo*  $^{13}\text{C}$  spectrum of the prostate with reasonably good signal-to-noise obtained using conventional  $^{13}\text{C}$  spectroscopy and a pelvic surface coil made by Medical Advances, Inc. (Milwaukee, WI) in a 1.5-T system. The data acquisition time was approximately 15 min (32). Based on this result, it may be possible to estimate the voxel size  $v$  in an CMRI/S experiment with enhanced S/N for a given scan time of 2 h. For a polarization transfer experiment  $v$  can be estimated as follows. If we suppose that the size of a typical prostate gland is  $36\text{ cm}^3$  from which the total citrate signal is derived, then  $v\eta/36 = 1/(120/15)^{1/2}$ , where  $\eta$  is the sensitivity enhancement factor which can be estimated conservatively to be at least 6. Based upon this,  $v$  is on the order of  $2\text{ cm}^3$ .

Finally, the problem of rf power deposition caused by proton decoupling has been examined recently by Heerschap *et al.* (33). Their data at 1.5 T showed that there is no evidence of excess SAR (that exceeds 4 W/kg) observed in their experiments by applying the Waltz-4 (34) decoupling scheme.

### REFERENCES

1. R. R. ERNST, G. BODENHAUSEN, AND A. WOKAUN, “Principles of Nuclear Magnetic Resonance in One and Two Dimensions.” Oxford Univ. Press (Clarendon), London/New York, 1987.
2. G. A. MORRIS AND R. FREEMAN, *J. Amer. Chem. Soc.* **101**, 760 (1979).

3. D. P. BURUM AND R. R. ERNST, *J. Magn. Reson.* **39**, 163 (1980).
4. D. M. DODDRELL, D. T. PEGG, AND M. R. BENDALL, *J. Magn. Reson.* **48**, 323 (1982).
5. M. R. BENDALL AND D. T. PEGG, *J. Magn. Reson.* **53**, 272 (1983).
6. T. R. BROWN, B. M. KINCAID, AND K. UGURBIL, *Proc. Natl. Acad. Sci. USA* **79**, 3523 (1982).
7. A. A. MAUDSLEY, S. K. HILAL, W. H. PERMAN, AND H. E. SIMON, *J. Magn. Reson.* **51**, 147 (1983).
8. D. W. KORMOS, H. N. YEUNG, AND R. C. GAUSS, *J. Magn. Reson.* **71**, 159 (1987).
9. D. W. KORMOS AND H. N. YEUNG, *Magn. Reson. Med.* **4**, 500 (1987).
10. L. O. SILLERUD, D. B. VAN HULSTEYN, AND R. H. GRIFFEY, *J. Magn. Reson.* **76**, 380 (1988).
11. H. N. YEUNG AND S. D. SWANSON, *J. Magn. Reson.* **83**, 183 (1989).
12. D. G. NORRIS, N. SCHUFF, AND D. LEIBFRITZ, *J. Magn. Reson.* **78**, 362 (1988).
13. M. H. LEVITT, R. FREEMAN, AND T. FRENKIEL, *Adv. Magn. Reson.* **11**, 47 (1983).
14. A. BAX, "Two-Dimensional Nuclear Magnetic Resonance in Liquids." Reidel, London, 1982.
15. R. G. SCHULMAN, T. R. BROWN, K. UGURBIL, S. OGAWA, S. M. COHEN, AND J. A. DEN HOLLANDER, *Science* **205**, 160 (1979).
16. K. WUTHRICH, "NMR in Biological Research: Peptides and Proteins." Elsevier, New York, 1976.
17. J. R. ALGER, L. O. SILLERUD, K. L. BEHAR, R. J. GILLIES, R. G. SHULMAN, R. E. GORDON, D. SHAW, AND P. E. HANLEY, *Science* **214**, 660 (1981).
18. L. O. SILLERUD AND R. G. SHULMAN, *Biochemistry* **22**, 1087 (1983).
19. C. H. HAN AND L. O. SILLERUD, *Magn. Reson. Med.* **3**, 626 (1986).
20. A. I. SCOTT AND R. L. BAXTER, *Annu. Rev. Biophys. Bioeng.* **10**, 151 (1981).
21. M. J. AVISON, H. P. HETHERINGTON, AND R. G. SHULMAN, *Annu. Rev. Biophys. Biophys. Chem.* **15**, 377 (1986).
22. L. O. SILLERUD, C. H. HAN, M. W. BITENSKY, AND A. A. FRANCENDESE, *J. Biol. Chem.* **261**, 4380 (1986).
23. W. E. HULL, M. ZERFOWSKI, AND P. BANNASCH, in "Book of Abstracts, Sixth Annual Meeting, Society of Magnetic Resonance in Medicine," p. 488, 1987.
24. S. M. COHEN, in "NMR Spectroscopy of Cells and Organisms" (R. K. Gupta, Ed.), Vol. I, p. 31. CRC Press, Boca Raton, FL, 1987.
25. S. M. COHEN, *Hepatology* **3**, 738 (1983).
26. L. C. COSTELLO, G. K. LITTLETON, AND R. B. FRANKLIN, in "Endocrine Control in Neoplasia" (R. K. Sharma and W. E. Criss, Eds.), p. 303. Raven Press, New York, 1978.
27. J. F. COOPER AND I. FARID, *J. Urol.* **92**, 533 (1964).
28. H. MARBERGER, E. MARBERGER, T. MANN, AND C. LUTWAK-MANN, *Brit. Med. J.* **1**, 835 (1962).
29. K. R. HALLIDAY, C. FENOGLIO-PREISER, AND L. O. SILLERUD, *Magn. Reson. Med.* **7**, 384 (1988).
30. K. UGURBIL, M. GARWOOD, A. R. RATH, AND M. R. BENDALL, *J. Magn. Reson.* **78**, 472 (1988).
31. L. O. SILLERUD, K. R. HALLIDAY, R. H. GRIFFEY, C. FENOGLIO-PREISER, AND S. SHEPARD, *Magn. Reson. Med.* **8**, 224 (1988).
32. L. O. SILLERUD, personal communication.
33. A. HEERSCHAP, P. R. LUYTEN, J. I. VAN DER HEIJDEN, AND J. DEN HOLLANDER, in "Book of Abstracts, Seventh Annual Meeting, Society of Magnetic Resonance in Medicine," p. 326, 1988.
34. A. J. SHAKA, J. KEELER, AND R. FREEMAN, *J. Magn. Reson.* **53**, 313 (1983).